SET readout using RF reflectometry and kinetic inductance nonlinearity

Jose Luis Montoya Agulló

Abstract

In this thesis we will make a proof of concept of a new type of charge sensor for quantum computation, using an SET, RF reflectometry and a kinetic inductance, which is the novel part of the sensor. First we will optimize the sensor analytically using a non-kinetic inductance, and then we will simulate the kinetic version to see if we can improve the fidelity. The results show that, for a non-kinetic sensor, the optimum tuning is done to the geometric mean of the two resistances we want to distinguish between, and that the use of a kinetic inductor with a proper calibration increases greatly the fidelity of the sensor, specially with parasitic resistances of the order of the smallest resistance.

Contents

1   Introduction

Silicon-based quantum computing is a quantum computing paradigm that uses trapped electrons in silicon quantum dots to build the qubits. The 3 main qubit architectures using QD are[1]:

- **Loss-DiVincenzo qubits:** Thought up by Loss and DiVincenzo[7] in their original paper, it defines the qubits as the spins of the trapped electrons themselves, and for their control uses a combination of an external magnetic field and the control of tunnel barriers between the QD.

- **Singlet-triplet qubits:** Proposed by Levy[6], instead of using single spins, it uses as basis the singlet and triplet state of a pair of spins. The main benefit with respect to the Loss-DiVincenzo is that the qubit lives in a decoherence-free subspace with respect to global magnetic fields that couple to the spin of the electron.

- **Exchange-only qubits:** Created by DiVincenzo *et al.*[2], it uses the spin of 3 QD to create a qubit fully controllable using voltages through the tunnel barriers that separate them.

The main advantage of silicon-based quantum computing is scalability, since it can leverage the decades in advancements of the CMOS industry. The objective with silicon-based quantum computing is then to build a quantum computer with an enormous amount of high fidelity qubits, instead of a quantum computer with a great amount of extremely high fidelity qubits, and to use the bigger number of qubits to run error correction algorithms. For this to be implemented, we need high fidelity and high speed readout techniques. At the moment there are multiple measuring schemes showing promising results[3], such as RF reflectometry of a SET. In this master's thesis, we will explore the use of a kinetic inductor in this measuring scheme with the objective of improving the performance.

2   Aims and objectives

As said in the previous section, the aim of this thesis is to explore the use of a kinetic inductor to improve the measurements on silicon spin qubits. The steps to take for this will be:

1. Learn the basics of: how a SET functions, RF reflectometry and kinetic inductance non-linearity.

2. Analyze a conventional measuring circuit to obtain expressions for the parameters and the contrast with an optimum configuration.

3. Explore the viability of using a kinetic inductor to improve the measuring performance of the previous circuit via numerical simulations.

3 Theoretical background

Before delving into the design and optimization of our measuring circuit, we need some theoretical context. First we will do a light overview of the operating principles of an SET and how to use it to measure spin, then we will pick a couple of concepts from RF reflectometry, and finally we will see that in the superconducting regime a new kind of inductance appears that depends on current.

3.1 The SET for spin sensing

Let's imagine a neutral conducting isolated island with capacitance C. If we want to stuff N electrons into it, the energy required would be

$$E = \frac{Q^2}{2C} = \frac{e^2}{2C} N^2 = E_C N^2$$

With the energy that the last electron needs being

$$E_N = E_C N^2 - E_C (N-1)^2 = E_C (2N-1)$$

So, due to Coulomb repulsion, a discrete energy spectrum appears with a gap $2E_C$. This separation of the energy levels is known as Coulomb blockade, because it blocks an electron (or charge in general, but we are interested in electron transport) from entering the island, unless it has enough energy to overcome the Coulomb repulsion due to the charges already inside (or in other words, enough energy to overcome that gap[1]).

A single electron transistor (SET for short) is a device that uses Coulomb blockade to, well, do what it says in the name: turning on or off a single electron current.

It consists of a conducting island connected to two voltage sources (V_s and V_d) via tunnel barriers (the common nomenclature is tunnel junctions, so from now on is how we are going to call them) and to a third voltage (V_g) via a capacitor C_C (figure 1). Each tunnel junction is modeled like a capacitor in parallel with a resistance, to model both the accumulation of charge at the walls and the current due to tunneling events respectively. Due to this function, the resistance needs to be high enough for each tunneling event to be well-defined in time.

To estimate the threshold for the resistance we can use the energy-time Heisenberg uncertainty principle

$$\Delta E \Delta t \geq \hbar/2$$

With the ΔE and Δt of the tunneling event. For ΔE we will use E_C, since it is the smallest variation in energy permitted in the island due to Coulomb blockade, and for Δt we will use the classical discharge time of a parallel RC circuit $\tau = RC$, which should be of the order of the time there is between tunneling events:

$$\Delta E \Delta t \geq \frac{\hbar}{2} \Rightarrow R \geq \frac{\hbar}{e^2}$$

---

[1]Technically speaking the electron also needs energy to overcome the energy gap due to quantum mechanical effects of the bulk, but since for a big enough island this gap is negligible in comparison with $2E_C$ [8], we are going to ignore it
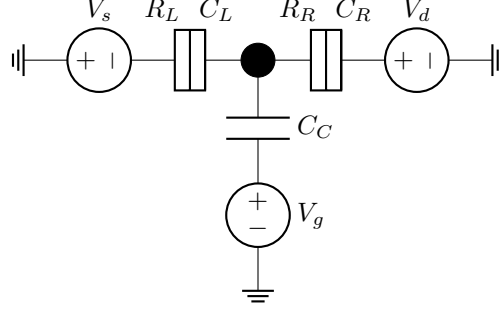
Figure 1: Circuit diagram of a SET. From left to right we have: the source voltage (V_s), the resistance and capacitance of the left tunnel junction (R_L, C_L), the capacitance of the central capacitor (C_C), the gate voltage (V_g), the resistance and capacitance of the right tunnel junction (R_R, C_R) and the drain voltage (V_d)

So, for the tunnel events occur with enough separation in time to be distinguishable, the resistance of the tunnel junction must be much bigger that $\hbar/e^2$

In reality, following a more rigorous analysis called orthodox theory one can arrive at a more restrictive condition for R[4]

$$R \gg \frac{h}{e^2} \approx 25.8\text{k}\Omega$$

With that out of the way we can begin to piece how does the SET manage to turn on and off a single electron current.

We begin with the electrostatic energy on the island, which is a combination of the charging energies of the capacitors and the work that the voltages have done to charge them

$$
\begin{aligned}
E_{el} &= \frac{1}{2}\left(\frac{q_L^2}{C_L} + \frac{q_C^2}{C_C} + \frac{q_R^2}{C_R}\right) - q_L V_s - q_C V_g - q_R V_d \\
&= \frac{1}{2}\left(C_L V_L^2 + C_C V_C^2 + C_R V_R^2\right) - C_L V_L V_s - C_C V_C V_g - C_R V_R V_d \\
&= \frac{1}{2}\left(C_L(V_L^2 - 2V_s V_L) + C_C(V_C^2 - 2V_g V_C) + C_R(V_R^2 - 2V_d V_R)\right) \\
&= \frac{1}{2}\left(C_L((V_L - V_s)^2 + V_s^2) + C_C((V_C - V_g)^2 + V_g^2) + C_R((V_R - V_d)^2 + V_d^2)\right)
\end{aligned}
$$

The next step is to obtain the values of V_L, V_C and V_R. For this, we just need to solve the system of equations comprised of two applications of Kirchhoff's voltage law

$$V_L + V_C = V_s + V_g$$
$$V_L + V_R = V_s + V_d$$

And the fact that the charge on the island is discrete

$$
\begin{aligned}
eN &= q_L - q_C - q_R \\
&= C_L V_L - C_C V_C - C_R V_R
\end{aligned}
$$

4

Which gives us the equality

$$V_L - V_s = -(V_C - V_g) = -(V_R - V_d) = \frac{eN - (C_L V_s - C_C V_g - C_R V_d)}{C_L + C_C + C_R}$$

Naming $C_\Sigma = C_L + C_C + C_R$ the total capacitance of the island and $q = C_L V_s - C_C V_g - C_R V_d$ as the induced charge in the quantum dot, we arrive at the expression of the electrostatic energy for the island in the SET

$$E(N) = E_C(N - q/e)^2 - \frac{1}{2}\left(C_L V_s^2 + C_C V_g^2 + C_R V_d^2\right) \text{ with } E_C = \frac{e^2}{2C_\Sigma}$$

The energy of the Nth electron in the island being then

$$E_N = 2E_C(N - 1/2 - q/e) \tag{3.1}$$

In order to analyze the behavior of the SET with N electrons inside, we need to know the energy variation of each possible single electron process, of which there are four: an electron gets out of the island through the left tunnel junction or through the right, or it gets into the tunnel junction through the left or through the right. The variation in energy with N electrons on the island is simply the energy of destination (voltage source/first empty energy level on the island) minus the energy of origin (voltage source/last full energy level on the island):

$$\Delta E_{IL}(N) = E_{N+1} - (-eV_s)$$
$$\Delta E_{OL}(N) = (-eV_s) - E_N$$
$$\Delta E_{IR}(N) = E_{N+1} - (-eV_d)$$
$$\Delta E_{OR}(N) = (-eV_d) - E_N$$

With IL/OL meaning in/out left and IR/OR meaning in/out right. Using 3.1

$$\Delta E_{IL}(N) = \quad 2E_C(N + 1/2 - q/e) + eV_s$$
$$\Delta E_{OL}(N) = -2E_C(N - 1/2 - q/e) - eV_s$$
$$\Delta E_{IR}(N) = \quad 2E_C(N + 1/2 - q/e) + eV_d$$
$$\Delta E_{OR}(N) = -2E_C(N - 1/2 - q/e) - eV_d$$

And with the simplifications $V_s = V$ and $V_d = 0$, a little bit of massaging, and using the definition of q, they turn into

$$\Delta E_{IL}(N) = \quad \frac{2E_C}{e(C_C + C_R)}\left(\frac{e}{C_C + C_R}\left(N + \frac{1}{2}\right) + V + \frac{C_C}{C_C + C_R}V_g\right)$$

$$\Delta E_{OL}(N) = -\frac{2E_C}{e(C_C + C_R)}\left(\frac{e}{C_C + C_R}\left(N - \frac{1}{2}\right) + V + \frac{C_C}{C_C + C_R}V_g\right)$$

$$\Delta E_{IR}(N) = \quad \frac{2E_C}{eC_L}\left(\frac{e}{C_L}\left(N + \frac{1}{2}\right) - V + \frac{C_C}{C_L}V_g\right)$$

$$\Delta E_{OR}(N) = -\frac{2E_C}{eC_L}\left(\frac{e}{C_L}\left(N - \frac{1}{2}\right) - V + \frac{C_C}{C_L}V_g\right)$$
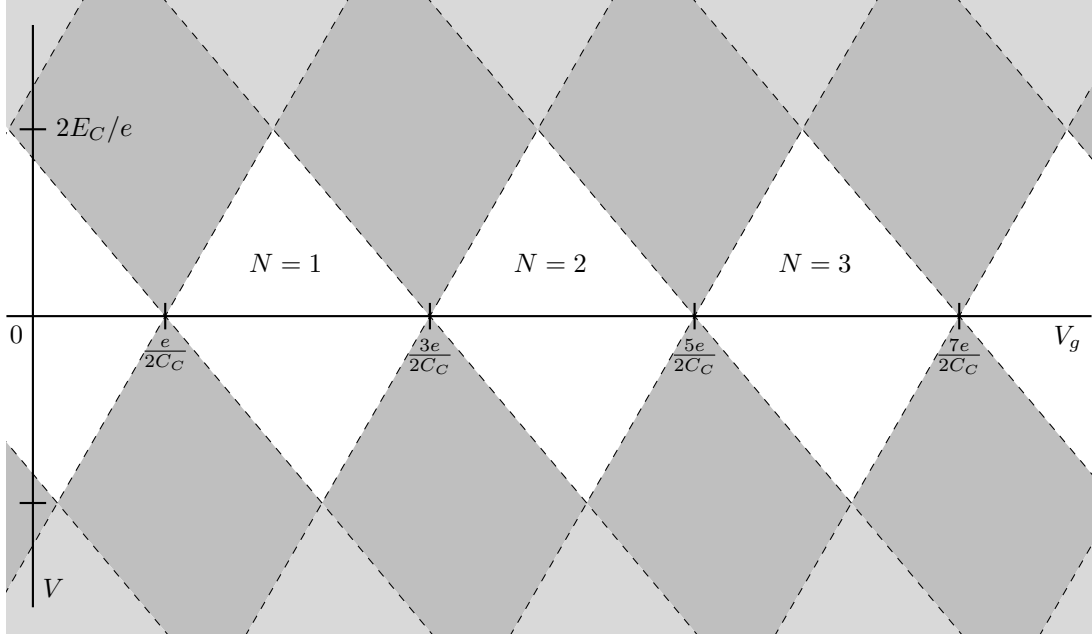
Figure 2: Coulomb diamonds in an SET due to Coulomb blockade. As we move towards the left, more charges are stored into the conducting island.

For a process to occur, the variation in energy of that process needs to be less than 0. Since we are interested in the transportation of charge through the SET, we want electrons flowing through one side to the other, which means $\Delta E_{IL}, \Delta E_{OR} < 0$ or $\Delta E_{IR}, \Delta E_{OL} < 0$. In figure 2 we can see a plot of this in the $V - V_g$ plane, with the white diamonds being where no condition is met, and darker diamonds being we are specifically $\Delta E_{IL}(N), \Delta E_{OR}(N+1) < 0$ and $\Delta E_{IR}(N), \Delta E_{OL}(N+1) < 0$.

With this we have enough information to have a basic understanding of how a SET works:

- For the SET to operate as it should, V needs to be lower than $2E_C/e$. If not, the current can not be turned off, and we cannot ensure that it is a one electron current. Picturing this scenario with the energy levels inside the conducting island it makes perfect sense. If $|V| > 2E_C/e$, the energy drop from one terminal to the other will be greater than the spacing between levels, ensuring that there is always an empty level to fill or a full level to empty.

- Using the same logic as the previous point, the thermal energy of the leads and the island must be smaller than E_C, since the thermal energy raises the available energy to mobilize while not increasing the required energy to move, giving effectively extra voltage to the system.

- The activation window for V_g is inversely proportional to V, and it occurs when thanks to V_g, an energy level is placed between 0 and V.

If we want to use a SET for spin sensing in a quantum dot, first we need to use it for charge

sensing. This is done by connecting via a capacitor the conducting island of the SET with the QD. When a charge is placed in the QD, it will influence the SET by, effectively, adding a bias to V_g. Choosing V and V_g appropriately for the bias that the charge introduces, we can tune the SET to make it let the current flow when a charge is present and stop it when it is absent (or the opposite).

For spin sensing, what we do is set up our system in such a way that the charge in the QD and the spin of that charge are correlated. This process is called spin to charge conversion, and there are mainly 2 ways of doing it:

- **Elzerman readout:** After inducing a Zeeman splitting in the QD, we can connect to it with a tunnel junction a reservoir, with a Fermi energy in between both spin states in the QD. If we detect a fluctuation in charge, it means the electron decayed through the reservoir to the lowest energy spin state. If not, it means it already was in the lowest energy spin state.

- **Pauli Spin Blockade:** By connecting to our QD another QD via a tunnel junction with lower energy and an electron with known spin, we can infer the spin in the first QD based on if a tunneling event occurred, thanks to the Pauli exclusion principle.

To summarize, a SET is a transistor that thanks to Coulomb blockade, a discretization on the energy spectrum of conducting islands due to Coulomb repulsion, is able to let a single electron current through and control it. It is main operation conditions are $e^2/C_\Sigma \gg V$ and $e^2/2C_\Sigma \gg k_b T$, with V the voltage applied, C_Σ the capacitance of the conducting island of the SET, k_b the Boltzmann constant and T the temperature of the SET, and when current flows, its resistance must be such that $R \gg 51.6\text{k}\Omega$.

By connecting a quantum dot to we can measure the charge inside it, and by implementing a spin to charge conversion scheme we can also measure the spin of said charge.
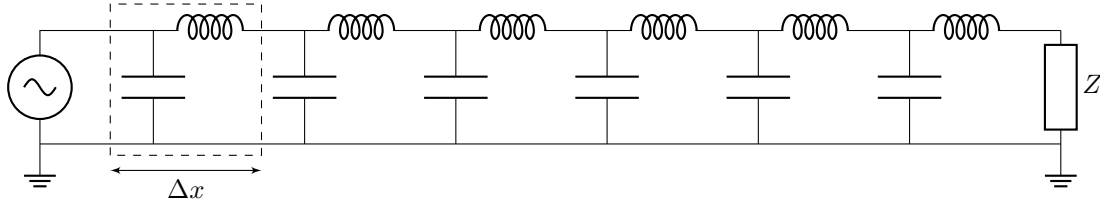
Figure 3: Lumped element model of a lossless transmission line connected to a generic impedance Z. In order to model the relevant impedance per unit length of the transmission line at radio frequencies, we represent it via sections with inductors in series and capacitors in parallel. Each periodic section like the one inside the dashed rectangle represents a segment of length Δx of the transmission line.

3.2 RF reflectometry

Radio frequency reflectometry is a method to measure change in an impedance connected to a transmission line via the reflection of a radio signal.

Usual lumped element treatment of AC circuits assumes that the size of the circuit is small with respect to the wavelength of the voltage, but with radio frequency voltages we cannot do that. The main consequences for us are:

- Now voltage and current are dependent on how far along the circuit you are, due to how fast it changes with respect to the size of the circuit itself $(V(t), I(t) \to V(x,t), I(x,t))$

- The intrinsic inductance and capacitance per unit length of a long connection cannot be ignored

In such cases those connections are made with what is known as a transmission line, which is a cable designed to minimize the radiation of power via that inductance and capacitance, and includes a signal and a ground connection in one package. One example of a transmission line would be a coaxial cable, in which the central conductor is the signal and the outer jacket ground.

Even though a transmission line minimizes that radiation of power, it does not erase it, and we need to take it into account in our calculations. To model this inductance and capacitance per unit length (L_l and C_l respectively), we will discretize it via a lumped element representation like in figure 3, ignoring the losses by not including any resistance in our circuit. Each pair inductor-capacitor will occur along a length Δx of the transmission line, so their inductance and capacitance in that stretch will be $L = \Delta x \cdot L_l$ and $C = \Delta x \cdot C_l$. Applying Kirchhoff at a point x in the transmission line we get

$$V(x + \Delta x, t) - V(x, t) = -\Delta x L_l \frac{\partial I}{\partial t}$$

$$I(x + \Delta x, t) - I(x, t) = -\Delta x C_l \frac{\partial V}{\partial t}$$

8

And doing the limit $\Delta x \to 0$ gives us the telegraph equations for a lossless transmission line

$$\frac{\partial V}{\partial x} = -L_l \frac{\partial I}{\partial t}$$
$$\frac{\partial I}{\partial x} = -C_l \frac{\partial V}{\partial t} \tag{3.2}$$

With solutions

$$V(x,t) = V_+(t - x/v_p) + V_-(t + x/v_p)))$$
$$I(x,t) = \frac{1}{Z_0}(V_+(t - x/v_p) - V_-(t + x/v_p))$$

Where $v_p = \frac{1}{\sqrt{L_l C_l}}$ is the phase velocity of the wave, $Z_0 = \sqrt{\frac{L_l}{C_l}}$ is the characteristic impedance of the line and V_+ and V_- are generic functions that describe a right and left traveling wave respectively. Since we will be choosing our reference frame such that our signal will be always traveling from left to right, the appearance of V_- in our calculations will mean a reflection.

If we add a generic impedance Z at the end of the transmission line, we add the boundary condition

$$\frac{V(x_{\text{End}}, \omega)}{I(x_{\text{End}}, \omega)} = Z(\omega)$$

With $V(x, \omega)$ and $I(x, \omega)$ being the time Fourier transforms of $V(x,t)$ and $I(x,t)$ respectively. Choosing $x = x_{\text{End}} = 0$ to simplify and using the time Fourier transforms of expressions 3.2, we get

$$\frac{V(0, \omega)}{I(0, \omega)} = Z_0 \frac{V_+(\omega) + V_-(\omega)}{V_+(\omega) - V_-(\omega)} = Z(\omega) \tag{3.3}$$

As we can see, the only way in which $Z_0 = Z(\omega)$ is if $V_{+,-}(\omega) = 0$, or in other words, the only way to not get a reflection is to match Z_0 to $Z(\omega)$. A useful parameter to define is the reflection coefficient $\Gamma = \frac{V_-(\omega)}{V_+(\omega)}$, and with equality 3.3 has the form

$$\Gamma = \frac{Z(\omega) - Z_0}{Z(\omega) + Z_0} \tag{3.4}$$

This reflection coefficient is the key to RF reflectometry, because if we know the characteristic impedance of our transmission line, we can measure the power and the phase reflected and obtain $Z(\omega)$.

If we want to measure 2 distinct impedances, and we want to maximize the reliability of our measure, the obvious way to do it would be to make the values of Γ be as separated as possible. A more formal way to express this idea is through the signal-to-noise ratio (SNR)[9] of the measurement

$$\text{SNR} = |\Delta\Gamma|^2 \frac{P_0}{P_N} \tag{3.5}$$

With P_0 and P_N the power of the signal and noise respectively and $\Delta\Gamma = \Gamma_B - \Gamma_A$ the difference in reflection coefficients between the two states to measure, whose modulus is what is called the contrast. If we want to improve our measurements, we need to increase our SNR.

3.3 Kinetic inductance and his nonlinearity

Due to the high mobility of the charge carriers in a super conductor, a phenomenon known as kinetic inductance emerges. This name comes from the fact that as opposed to a usual inductor, which functions by storing energy in the magnetic field generated by the charge carriers, it is stored as the kinetic energy of the charge carriers themselves.

With this simple definition of the kinetic inductance and a little bit of Drude and Ginzburg-Landau theory, we have all we need to derive the property that interests us the most: it's nonlinearity.

The energy stored by an inductor of inductance L is

$$E = \frac{1}{2}LI^2$$

So, in the case of the kinetic inductance of length l and cross-section S

$$E_k = \frac{1}{2}L_k I^2 = \frac{1}{2}m(nlS)v^2$$

With n, m and v the volumetric density, the mass and the speed of the charge carriers. By solving for L_k and defining the volumetric current density as $j = nqv$ with q the charge of the charge carriers we arrive at the following expression

$$L_k = \frac{mlj^2}{nq^2Sj^2} = \frac{ml}{q^2S}\frac{1}{n}$$

Now, using the Ginzburg-Landau expression for the volumetric density of supercharge carriers

$$n(v) = |\Psi|^2 = \frac{1}{\beta}\left[|\alpha| - \frac{1}{2}mv^2\right]$$

And doing a second order approximation of L_k at $v \approx 0$, we arrive at our desired expression

$$L_k = L_{k0}\left(1 + \frac{j^2}{j_*^2} + \dots\right) \tag{3.6}$$

With $L_{k0} = \frac{ml}{q^2Sn(v=0)}$ and $j_*^2 = \frac{2q^2|\alpha|^3}{m\beta^2}$. If we compare j_* to the critical current j_c, which is the maximum current that the system can withstand and can be calculated by obtaining the maximum of j with respect to v, we get that

$$j_* = \sqrt{\frac{27}{4}}j_c$$

With this we can not only see that the kinetic inductance has a quadratic dependence with the current, but that the sensibility of that dependence it is given by the critical current of the material.

But, the applications of inductors are usually with AC voltages, and in that case our kinetic inductance would be varying constantly. How can we use the kinetic inductor then?

The solution is to introduce a DC bias to the circuit, with an intensity much greater than the maximum of the AC current, but still small enough to not break superconductivity and to use an AC current much smaller than the critical current. With it, we can have an inductor that changes inductance along with the resistance of the SET, since the effects of the AC current can be ignored.

$$
\begin{aligned}
L_k &= L_{k0} \left(1 + \frac{(j_{AC} + j_{DC})^2}{j_*^2} + \dots \right) \\
&= L_{k0} \left(1 + \frac{j_{DC}^2}{j_*^2} + \frac{j_{DC} j_{AC}}{j_*^2} + \frac{j_{AC}^2}{j_*^2} + \dots \right) \\
&= L_{k0} \left(1 + \frac{j_{DC}^2}{j_*^2} + (\frac{j_{DC}}{j_*} + \frac{j_{AC}}{j_*}) \frac{j_{AC}}{j_*} + \dots \right) \\
&= L_{k0} \left(1 + \frac{j_{DC}^2}{j_*^2} + \dots \right) \text{ since } j_{DC} < j_c \text{ and } j_{AC} \ll j_c
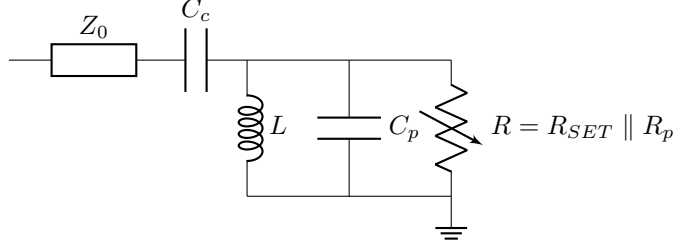\end{aligned}
$$

Figure 4: Topology of our measuring circuit. Since during most of our analysis we will ignore R_p, it is already couplet to R_{SET}.

4   Results

As we said in section 3.2, in RF reflectometry we use the reflection coefficient Γ (3.4) to measure an impedance $Z(\omega)$, and if said impedance can have two possible values, the relevant parameter to determine the distinguishability of those measures is the signal-to-noise ratio SNR (3.5).

Since $Z(\omega)$ can't be modified (it defeats the purpose of measuring it), and Z_0 depends on the transmission line (it usually is 50Ω), the standard procedure is to add a matching network (essentially, extra circuitry around $Z(\omega)$) and instead measure the impedance of said network plus $Z(\omega)$. The idea is that with the matching network we bring the impedance of the ensemble closer to Z_0, increasing the variation of Γ with respect to the impedance we want to measure, and with it improving our SNR via the contrast.

In our case, the impedance to measure is the resistance of the SET (R_{SET}), which has 2 states: $R_{\text{On}}^{SET} = 50\text{k}\Omega$[2] and $R_{\text{Off}}^{SET} = \infty\Omega$ (zero current passes). For our matching network, since $R_{SET} \gg Z_0$ we will use the appropriate version of what is known as a high pass L matching network. It consists of a coupling capacitance C_c connected in series with Z_0 and R_{SET}, and an inductance L in series with R_{SET}. In figure 4 we can see this arrangement with the addition of a parasitic capacitance and resistance, C_p and R_p, which are used to model the losses in the circuit. Due to its shape, we will refer to it as the parallel RLC resonator, or the resonator for short.

The objectives of this section are to first study our measuring circuit, find the optimal values of its parameters, and see what that ideal measurement would look like, while along the way keep doing simulations to ensure that our results work. Next, we will check if with a kinetic inductor the performance can be improved, and under what circumstances said improvement occurs.

---

[2]I know that in section 3.1 we saw that it must be a lot greater than $51.6\text{k}\Omega$, but we're going to work in a worst case scenario

4.1 The parallel RLC resonator

4.1.1 Resonant frequency and effective impedance

Our analysis begins with obtaining expressions for the resonant frequency and the effective impedance of our resonator. It's easy to see that its impedance is

$$Z(\omega) = \frac{1}{j\omega C_p + \frac{1}{j\omega L} + \frac{1}{R}} + \frac{1}{j\omega C_c} \tag{4.1}$$

Which after a little massaging turns into

$$Z(\omega) = \frac{\omega^2 L^2 R}{R^2(1 - \omega^2 C_p L)^2 + \omega^2 L^2} + j\left(\frac{\omega L R^2(1 - \omega^2 C_p L)}{R^2(1 - \omega^2 C_p L)^2 + \omega^2 L^2} - \frac{1}{\omega C_c}\right)$$

The resonant frequency ω_r that makes $\mathrm{Im}\, Z(\omega) = 0$ is

$$\omega_r^2 = \frac{1}{L(C_c + C_p)}\left(1 + \frac{C_c}{2C_p} - \frac{L}{2R^2 C_p} \pm \sqrt{\left(1 + \frac{C_c}{2C_p} - \frac{L}{2R^2 C_p}\right)^2 - 1 - \frac{C_c}{C_p}}\right)$$

Choosing C_c and L such that $\frac{C_c}{C_p}, \frac{L}{R^2 C_p} \ll 1$, leaves us with the approximate expression for the resonant frequency

$$\omega_r \approx \frac{1}{\sqrt{L(C_c + C_p)}} \tag{4.2}$$

Finally, to obtain the effective impedance we use this expression in $\mathrm{Re}\, Z$

$$Z_{eff} = \mathrm{Re}\, Z(\omega_r) = \frac{\omega_r^2 L^2 R}{R^2(1 - \omega_r^2 C_p L)^2 + \omega_r^2 L^2} \approx \frac{L(C_c + C_p)}{RC_c^2}\left(1 + \frac{L(C_c + C_p)}{R^2 C_c^2}\right)^{-1}$$

And by, again, choosing L and C_c such that $\frac{L(C_c + C_p)}{R^2 C_c^2} \ll 1$ we arrive to our expression for the effective impedance

$$Z_{\text{eff}} \approx \frac{L(C_c + C_p)}{RC_c^2} \tag{4.3}$$

During the optimization of the resonator we will be using quite a lot of expressions obtained via approximations in non-approximated systems, only to do more approximations with them. Due to this, it is really important to have a clear picture of the regimes we are working in to ensure that our results work in the state-of-the-art technology, and that is why after each result we are going to recontextualize our approximations.

In this case, the approximations to obtain ω_r are clear and straight forward:

$$\frac{C_c}{C_p} \ll 1 \tag{4.4}$$

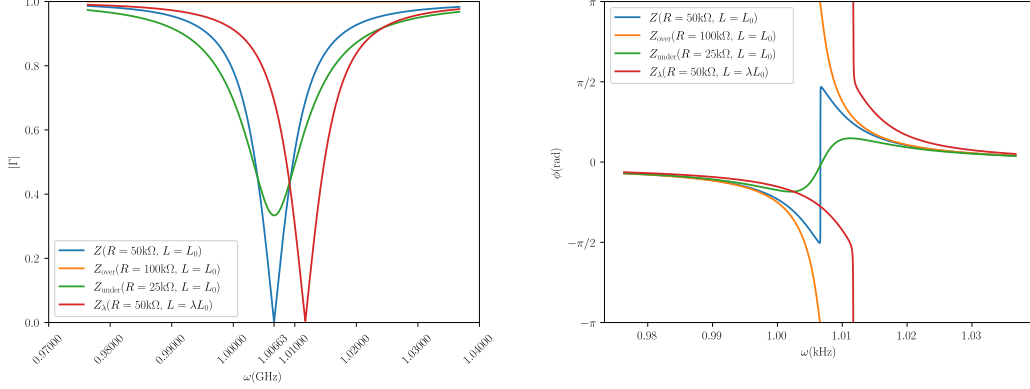$$\frac{L}{R^2 C_p} \ll 1 \tag{4.5}$$

Figure 5: Modulus and phase of Γ in multiple configurations. $Z_0 = 50\Omega$, $C_p = 500\text{fF}$, $C_c = 100\text{fF}$, $L = 41.67\text{nH}$. The script generating this image can be found in the companion Github repository with the name `ReflecGraph.py`.

But the approximation for Z_{eff} needs a little bit of extra work. If we multiply $(C_c/C_p)^2$ in both sides, it turns into

$$\frac{L}{R^2 C_p}\left(1 + \frac{C_c}{C_p}\right) \ll \left(\frac{C_c}{C_p}\right)^2 \qquad (4.6)$$

And since we used equation 4.2 to arrive here, it must hold the approximation 4.4, turning the previous expression into

$$\frac{L}{R^2 C_p} \ll \left(\frac{C_c}{C_p}\right)^2 \qquad (4.7)$$

While approximations 4.4 and 4.5 impose a general condition in our degrees of freedom, approximation 4.7 imposes a relative condition between the previous two.

For checking that our results are correct, we can graph the modulus Γ as a function of the voltage frequency ω. With the parameters listed in figure 5, the 3 conditions for our approximations are met, and with a resistance $R = 50\text{k}\Omega$ (so $R_p = \infty\Omega$), $Z_{\text{eff}} \approx Z_0$ around $\omega_r = 1.00654\text{GHz}$. This means that $|\Gamma|$ should dip to 0 quickly around ω_r, which is exactly what we see.

In addition to this configuration, we have also graphed the reflection coefficient of the same resonator, but with variations in the resistance ($R = 2R_{\text{On}}$ and $R = R_{\text{On}}/2$) and a slight variation in the inductance (99% of the previous one). The variation of the resistance serves as an example of a behavior that we will observe later: even though they are not the same distance in R space from the resonant resistance, they are in Γ space, with directly opposing positions in the complex plane as can be seen in the phase graph. This is because, while in resonance, the distance in Γ space does not depend on the distance in R space, it depends on the relative distance, with

14

the direction determined by which resistance (the resonant or the perturbed one) is bigger. The variation in the inductance serves as another way of creating distance between two values of Γ, and our hope is that it can work alongside a resistance change.

4.1.2 Contrast and optimization

With an expression for the effective impedance of the system in resonance and an expression for the resonant frequency, we can begin the search for the optimum parameters of the circuit. Or in other words, what combination of parameters will yield the greatest contrast, and in turn the greatest SNR.

Since the values of the parameters used on the circuit of figure 5 are of the same order of magnitude as the ones used in the lab for similar circuits[5], it is safe to assume that the values of L and C_c will be of the around the same size. With this in mind is easy to see that our approximation of ω_r will be a lot more sensible to changes in L than to changes in C_c, and thus we will use C_c to optimize the contrast, while we will use L to ensure that we stay in an acceptable frequency of operation.

We begin obtaining a workable expression of the contrast by plugging

$$\omega = \frac{1}{\sqrt{L(C_c + C_p)}}$$

into 4.1:

$$
\begin{aligned}
Z(\omega) &= \frac{1}{j\omega C_p + \frac{1}{j\omega L} + \frac{1}{R}} + \frac{1}{j\omega C_c} \\
&= \frac{\omega RL}{R(1 - \omega^2 LC_p) + j\omega L} + \frac{1}{j\omega C_c} \\
&= \frac{\frac{jRL}{\sqrt{L(C_c+C_p)}}}{R\left(1 - \frac{\cancel{L}C_p}{\cancel{L}(C_c+C_p)}\right) + \frac{jL}{\sqrt{L(C_c+C_p)}}} + \frac{\sqrt{L(C_c + C_p)}}{jC_c} \\
&= \frac{jRL}{R\sqrt{L(C_c + C_p)}\left(\frac{C_c}{C_c+C_p}\right) + jL} + \frac{\sqrt{L(C_c + C_p)}}{jC_c} \\
&= \frac{jR\cancel{L}}{R\frac{\cancel{L}(\cancel{C_c+C_p})}{\sqrt{L(C_c+C_p)}}\left(\frac{C_c}{\cancel{C_c+C_p}}\right) + j\cancel{L}} + \frac{\sqrt{L(C_c + C_p)}}{jC_c} \\
&= \frac{jR}{RS + j} + \frac{1}{jS} = \frac{\cancel{-RS} + \cancel{RS} + j}{jRS^2 - S} = \frac{1}{RS^2 + jS} \text{ with } S = \frac{C_c}{\sqrt{L(C_c + C_p)}}
\end{aligned}
\tag{4.8}
$$

Using this expression to obtain the reflection coefficient, but using the admittance of the

15

transmission line instead of the impedance ($Y_0 = 1/Z_0$) yields

$$\begin{aligned} \Gamma &= \frac{Z(\omega) - Z_0}{Z(\omega) + Z_0} = \frac{Y_0 - 1/Z(\omega)}{Y_0 + 1/Z(\omega)} \\ &= \frac{2Y_0}{Y_0 + 1/Z(\omega)} - 1 = \frac{2Y_0}{RS^2 + Y_0 + jS} - 1 \\ &= 2Y_0 \frac{RS^2 + Y_0 - jS}{(RS^2 + Y_0)^2 + S^2} - 1 \end{aligned}$$

Since $\omega \approx \omega_r$ then $\operatorname{Im} Z(\omega) \approx 0$ and by extension $\operatorname{Im} \Gamma \approx 0$, so

$$\Gamma \approx 2Y_0 \frac{RS^2 + Y_0}{(RS^2 + Y_0)^2 + S^2} - 1$$

Next, using the parameters utilized for figure 5 to get a sense of the scale, it is safe to assume that the following approximation is correct

$$(RS^2 + Y_0)^2 \gg S^2 \tag{4.9}$$

Which leaves us with the following expression for the reflection coefficient

$$\Gamma \approx \frac{2Y_0}{RS^2 + Y_0} - 1$$

And this one for the contrast

$$|\Delta\Gamma| = |\Gamma(R = R_{\text{Off}}) - \Gamma(R = R_{\text{On}})| \approx 2Y_0 \left| \frac{1}{R_{\text{Off}}S^2 + Y_0} - \frac{1}{R_{\text{On}}S^2 + Y_0} \right|$$

Now, thanks to this simplified form of the contrast, to obtain the optimum value for C_c we don't need any fancy tricks, just to derive with respect to C_c and equate to 0. Doing this we arrive at the equation

$$S^2 = \frac{Y_0}{\sqrt{R_{\text{Off}}R_{\text{On}}}} \tag{4.10}$$

And solving it for C_c, we get the single solution (for $R_{\text{On}}, R_{\text{Off}}, Y_0, L, C_p, C_c \geq 0$)

$$C_{c\text{Max}} = \frac{LY_0}{2\sqrt{R_{\text{Off}}R_{\text{On}}}} \left(1 + \sqrt{1 + 4C_p \frac{\sqrt{R_{\text{Off}}R_{\text{On}}}}{LY_0}} \right) \tag{4.11}$$

We could simply plug this result into a simulation and call it a day, but with a little bit more digging we can extract some interesting results.

First off, by the way the resistances appear in 4.10 and 4.11 it leads really naturally to defining a ratio parameter

16

$$\rho = \frac{R_{\text{Off}}}{R_{\text{On}}} \geq 1$$

With it our expressions 4.10 and 4.11 turn to

$$S^2 = \frac{Y_0}{\sqrt{\rho}R_{\text{On}}} \tag{4.12}$$

$$C_{c\text{Max}} = \frac{LY_0}{2\sqrt{\rho}R_{\text{On}}} \left(1 + \sqrt{1 + 4C_p \frac{\sqrt{\rho}R_{\text{On}}}{LY_0}}\right)$$

Then, by using the definition of S from 4.8 and using impedance, we can rearrange 4.12 to

$$Z_0 = \frac{L(C_c + C_p)}{\sqrt{\rho}R_{\text{On}}C_c^2}$$

Which is what we saw in figure 3.4 with the variations in resistance: When tuning the resonator to the geometric mean of the resistances of the two states, the reflection coefficients end up in opposing sides of 0 within the real line. What this result shows is that this is the optimum arrangement.

In addition to this insight, we can also use 4.12 in our approximation for the contrast (4.9) to see that, when optimized, it only depends on the ratio of the resistances (or the ration between the resistances and the tuning resistance), and that it has a maximum value of 2, which is expected:

$$|\Delta\Gamma| \approx 2Y_0 \left|\frac{1}{R_{\text{Off}}S^2 + Y_0} - \frac{1}{R_{\text{On}}S^2 + Y_0}\right| = 2\left|\frac{1}{\sqrt{\rho}+1} - \frac{\sqrt{\rho}}{1+\sqrt{\rho}}\right| = 2\left|\frac{1-\sqrt{\rho}}{1+\sqrt{\rho}}\right| \tag{4.13}$$

After these results it seems appropriate to analyze with more detail the approximations used, so we can contextualize the regime in which this works. The first approximation done was $\omega \approx \omega_r$, which boils down to 4.5 and 4.4. The second approximation was 4.9, so let's see if with the optimum C_c it holds. Using 4.12 we have

$$(RS^2 + Y_0)^2 \gg S^2 \rightarrow \left(\frac{RY_0}{\sqrt{\rho}R_{\text{On}}} + Y_0\right)^2 \gg \frac{Y_0}{\sqrt{\rho}R_{\text{On}}}$$

Now, considering $R = R_{\text{On}}$ since it's the worst case scenario and returning to the use of impedance instead of admittance, the condition turns to

$$\left(\frac{1}{\sqrt{\rho}} + 1\right)^2 \gg \frac{Z_0}{\sqrt{\rho}R_{\text{On}}}$$

Finally, we can use the worst possible value of ρ on each side ($\rho = 1$ for the right side and $\pi = \infty$ for the left) and arrive at

$$R_{\text{On}} \gg Z_0 \tag{4.14}$$

Now that we have finished our calculations, it is time to introduce the parasitic resistance. This is important because it depends on the design of the circuit, and plotting $|\Delta\Gamma|(R_p)$ will tell us with want amount of losses we can get our results.

To introduce it we will give it the same treatment to R_p as to R_{Off} by introducing a ratio parameter

$$\pi = \frac{R_p}{R_{\text{On}}^{SET}}$$

With the important distinction that, as opposed to ρ, $0 \leq \pi \leq \infty$, with $\pi = 0$ being a short circuit and $\pi = \infty$ being a lossless circuit.

The substituions are then

$$R_{\text{On}} = \frac{\pi}{1+\pi} R_{\text{On}}^{SET}$$
$$R_{\text{Off}} = \frac{\rho_{SET}\pi}{\rho_{SET}+\pi} R_{\text{On}}^{SET}$$
$$\rho = \frac{\rho_{SET}(1+\pi)}{\rho_{SET}+\pi}$$

With $\rho_{SET} = R_{\text{Off}}^{SET}/R_{\text{On}}^{SET}$. Taking this even further beyond with the fact that in an SET $\rho_{SET} \approx \infty$ (in the off state, no electrons are travelling through), the substitutions are

$$R_{\text{On}} = \frac{\pi}{1+\pi} R_{\text{On}}^{SET}$$
$$R_{\text{Off}} = \pi R_{\text{On}}^{SET}$$
$$\rho = 1 + \pi$$

The introduction of the parasitic resistance and an infinite R_{Off}^{SET} doesn't change much, in the sense that for most of the expressions is better to simply use ρ and R_{On} for clarity. Most. Because for two results in specific it helps: in 4.13

$$|\Delta\Gamma| \approx 2 \left| \frac{1 - \sqrt{1+\pi}}{1 + \sqrt{1+\pi}} \right| \tag{4.15}$$

And in 4.14

$$\frac{\pi}{1+\pi} R_{\text{On}}^{SET} \gg Z_0 \rightarrow \pi \gg \frac{Z_0}{R_{\text{On}}^{SET} - Z_0} \tag{4.16}$$

Using the values of Z_0 and R_{On}^{SET} that we have been considering up until now (50Ω and $50k\Omega$ respectively) we can see that for 4.14 to work in a worse case scenario, π must be a lot greater
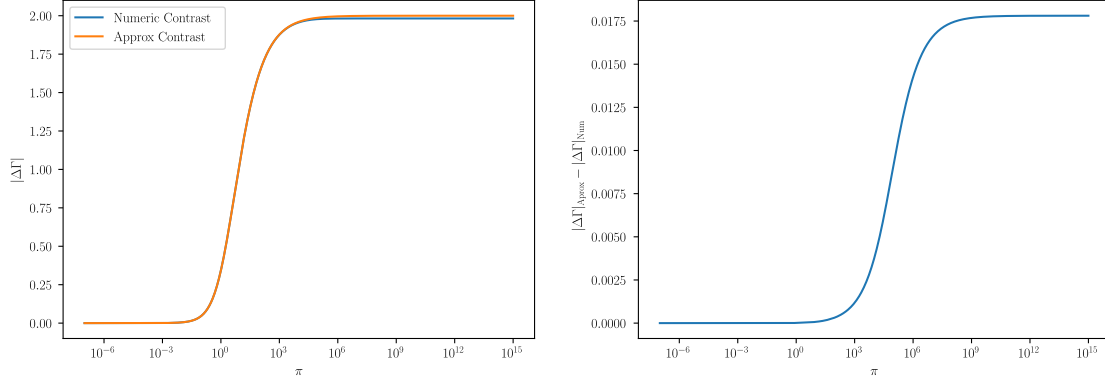
18

Figure 6: Numerical optimum contrast and our formula (4.15) with the difference between them. $L = 180\text{nH}$, $C_p = 500\text{fF}$, $Z_0 = 50\Omega$, $R_{\text{On}}^{SET} = 50\text{k}\Omega$, $\rho = 2 \cdot 10^6$. The script generating these images can be found in the companion Github repository with the name `OptContrComparison.py`

than 10^{-3}. It probably would be, given that for a π 100 times greater, $|\Delta\Gamma| \approx 0.0477$, which isn't a good contrast to aim for.

Finally, we check our results by comparing them against the numerically calculated optimum contrast via a simulation that searches the optimum value of C_c for a given value of π.

As we can see in figure 6, our estimations for what values of π were completely off, but in a good way. That is because even though the approximation gets worse for greater π, it caps off at 0.0175, which is negligible in comparison to the values of $|\Delta\Gamma|$ that we are aiming to.

To summarize, we have found the expression for the value of C_c that optimizes the contrast. This value effectively tunes the resonator to the geometric mean of the 2 possible resistances of the circuit, and makes the contrast depend on only in their ratio. All of this was found with the constraints 4.5, 4.4 and 4.1.2.

4.2 The parallel kinetic RLC resonator

Now that we have familiarized ourselves with the way a parallel RLC resonator behaves and how we can optimize it for the best possible contrast, we are going check with simulations if the introduction of a kinetic inductor can bring us any improvement in the measurement performance.

Like with the resistance, the SET letting current flow will be linked with an inductance L_{On}, and an inductance L_{Off} with the blocking of current. Taking a page out of the previous section, we are going to introduce a parameter λ defined as

$$\lambda = \frac{L_{\text{Off}}}{L_{\text{On}}} \leq 1$$

The reason that $\lambda \leq 1$ is that, since $R_{\text{On}} < R_{\text{Off}}$ and the voltage is constant, it means that $I_{\text{On}} > I_{\text{Off}}$, which with expression 3.6 we arrive that $L_{\text{On}} \leq L_{\text{Off}}$.

Since this part of the thesis is just to test the idea of using a kinetic inductance to improve

the readout, we will have the variation of R_{SET} and L decoupled for simplicity's sake.

The next thing we need to cover is a new problem that comes with a variable inductance: which one do we use for the frequency? Since we don't know which one is best, we'll introduce the parameter $1 \leq \lambda_t \leq \lambda$ such that $\omega = \frac{1}{\sqrt{\lambda_t L_{\text{On}}(C_c + C_p)}}$. This parameter will determine the tuning we will be using, which will boil down to 3:

- L_{On} tuning ($\lambda_t = 1$)

- L_{Off} tuning ($\lambda_t = \lambda$)

- Middle tuning ($1 < \lambda_t < \lambda$)

We won't consider the outside of this interval of frequencies because as we shall see it's objectively worse than any of these 3 options.

Before we begin with the simulations, I would like to briefly disclose why we did not try to obtain an analytical expression like in the previous subsection.

The reasoning can be easily seen by reproducing the first step in subsubsection 4.1.2, but with $\omega(\lambda_t)$ instead of ω and by using λL instead of L in the expression for the impedance[3]:

$$
\begin{aligned}
Z &= \frac{1}{j\omega(\lambda_t)C_p + \frac{1}{j\omega(\lambda_t)\lambda L_{\text{On}}} + \frac{1}{R}} + \frac{1}{j\omega(\lambda_t)C_c} \\
&= \frac{\omega(\lambda_t)R\lambda L_{\text{On}}}{R(1 - \omega(\lambda_t)^2 \lambda L_{\text{On}} C_p) + j\omega(\lambda_t)\lambda L_{\text{On}}} + \frac{1}{j\omega(\lambda_t)C_c} \\
&= \frac{R\lambda L_{\text{On}}}{\frac{R}{\omega(\lambda_t)}(1 - \omega(\lambda_t)^2 \lambda L_{\text{On}} C_p) + j\lambda L_{\text{On}}} + \frac{1}{j\omega(\lambda_t)C_c} \\
&= \frac{jR\lambda L_{\text{On}}}{\frac{R\omega(\lambda_t)}{\omega(\lambda_t)^2}\left(1 - \frac{\lambda L_{\text{On}} C_p}{\lambda_t L_{\text{On}}(C_c + C_p)}\right) + j\lambda L_{\text{On}}} + \frac{1}{j\omega(\lambda_t)C_c} \\
&= \frac{jR\lambda L_{\text{On}}}{R\omega(\lambda_t)\lambda_t L_{\text{On}}(C_c + C_p)\left(\frac{\lambda_t(C_c + C_p) - \lambda C_p}{\lambda_t(C_c + C_p)}\right) + j\lambda L_{\text{On}}} + \frac{1}{j\omega(\lambda_t)C_c} \\
&= \frac{jR\lambda L_{\text{On}}}{R\omega(\lambda_t)L_{\text{On}}\lambda\left(\frac{\lambda_t}{\lambda}(C_c + C_p) - C_p\right) + j\lambda L_{\text{On}}} + \frac{1}{j\omega(\lambda_t)C_c} \\
&= \frac{jR}{R\omega(\lambda_t)\left(\frac{\lambda_t}{\lambda}(C_c + C_p) - C_p\right) + j} + \frac{1}{j\omega(\lambda_t)C_c}
\end{aligned}
$$

We can see that, as opposed to the previous section, we can't wrap neatly C_c, C_p and L in a parameter like S. Due to this, I believe that to obtain an expression like the one for the non-kinetic resonator it would be necessary to do an analysis on a case by case basis with more context about the application to better choose the correct approximations, if arriving at a nice and practical expression is even possible that is. Since one of the objectives of this master's thesis is just to explore the viability of the use of a kinetic inductor, simulations and their analysis will suffice.

---

[3]This allows us to get Z_{On} with $\lambda = 1$ or Z_{Off} with $\lambda = \lambda$.
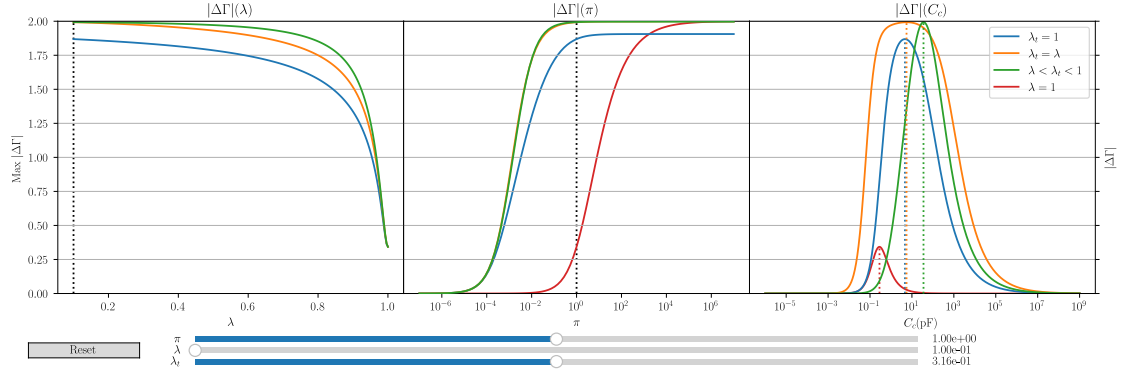
Figure 7: Multiple representations of the contrast with sliders to control their parameters. Right: $|\Delta\Gamma_{\mathrm{Opt}}(\lambda)|$. Center $|\Delta\Gamma_{\mathrm{Opt}}(\pi)|$. Left: $|\Delta\Gamma(C_c)|$. The script generating these images can be found in the companion Github repository with the name `IdealContrastOfRp&Lf&Cc.py`

4.2.1 Simulation of the effect on kinetic inductance on the contrast

In a simulation you have supreme control over what is simulated, how is simulated and what and how results are shown. A great deal of time was spent deciding these things, and the final decisions and their reasoning are the following:

The main value we are going to calculate and graph is $\Delta\Gamma(Z_0, \rho, R_{\mathrm{On}}, C_p, L_{\mathrm{On}}, \lambda_t, \pi, C_c, \lambda)$.

Due to the high number of inputs, we need to fix some of them in order to analyze in the best way possible how does $\Delta\Gamma$ behave. Taking inspiration from the non-kinetic case, in which for the optimum value of C_c the only parameter that affected the contrast was π, we will fix the following variable with the following values

Z_0	ρ	R_{On}	C_p	L_{On}
50Ω	$2 \cdot 10^6$	$50\mathrm{k}\Omega$	$500\mathrm{fF}$	$180\mathrm{nH}$

So, what we will graph is $\Delta\Gamma(\lambda_t, \pi, C_c, \lambda)$, which only depends on π, C_c (since we'll need to find the optimal value numerically), and all the new variables associated with the introduction of a variable inductance. This still leaves us with a 4 variable function, and the best way to plot it that I could think of can be seen in figure 7

In the left and central plot we have the modulus of $\Delta\Gamma_{\mathrm{Opt}}$, which is $\Delta\Gamma$ with the value of C_c that maximizes the modulus, as a function of λ and π respectively, and the left plot is $|\Delta\Gamma(C_c)|$. In each there are multiple lines: 3 with a different value of λ_t and one with $\lambda = 1$ to act as reference for the non-kinetic case (for the left plot it didn't make sense to add the reference line). Finally, we have 3 sliders to control the plots in real time:

- π slider controls the value of π for the left and right plot, and the dotted black line in the center plot

- λ slider controls the value of λ for the center and right plot, and the dotted black line in
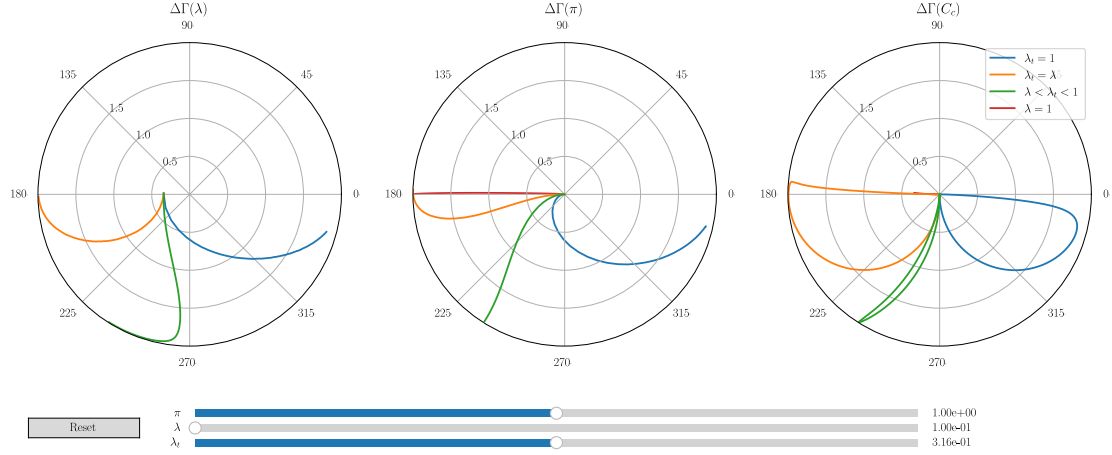
21

Figure 8: Multiple representations of the contrast with sliders to control their parameters. Right: $\Delta\Gamma_{\text{Opt}}(\lambda)$. Center $\Delta\Gamma_{\text{Opt}}(\pi)$. Left: $\Delta\Gamma(C_c)$. The script generating these images can be found in the companion Github repository with the name `IdealContrastOfRp&Lf&CcComplexPlane.py`

the left plot

- λ_t slider controls the value of λ_t for the plot with $\lambda < \lambda_t < 1$

The range of the λ and π sliders is the same as the domain of the respective plots ($\lambda \in [0.1, 1]$, $\pi \in [10^{-7}, 10^7]$), and the range of the λ_t slider is $\lambda_t \in [\lambda, 1]$ (the edges were included, so it could be seen how it morphs into the other two plots). The starting values of each slider are $\pi = 1$, $\lambda = 0.1$ and $\lambda_t = \sqrt{\lambda}$. The domain of the right plot is $C_c \in [10^{-18}, 10^{-3}]$fF, and it was chosen such that for any combination of λ and π the maxima was in it, since it is also the range in which the simulation search for the optimum C_c.

The main observations, both in relevance and notoriety, can be seen directly with figure 7

- A smaller λ is always better in order to improve the contrast

- λ_t and $\lambda < \lambda_t < 1$ are objectively better than the non-kinetic case, with the main difference being that with an intermediate λ_t the optimum C_c is greater

- $\lambda_t = 1$ hits a ceiling that causes that, for a high enough value of π, the introduction of a kinetic inductor is actually worse than a non-kinetic one. With the π slider can be seen that this ceiling depends on λ, but modifying the non-variable parameters shows that it also depends on them. To be more specific, $|\Delta\Gamma(\lambda_t = 1)| \propto R_{\text{On}}, C_p, 1/L_{\text{On}}$, with R_{On} being the more sensible of the 3 by a margin.

Thanks to the sliders a more thorough analysis of the simulation can be made, but nothing besides the previous points can be seen except for some quirky behavior not drastic enough to necessitate images, but curious enough to talk about it and encourage playing with the simulation to see it.
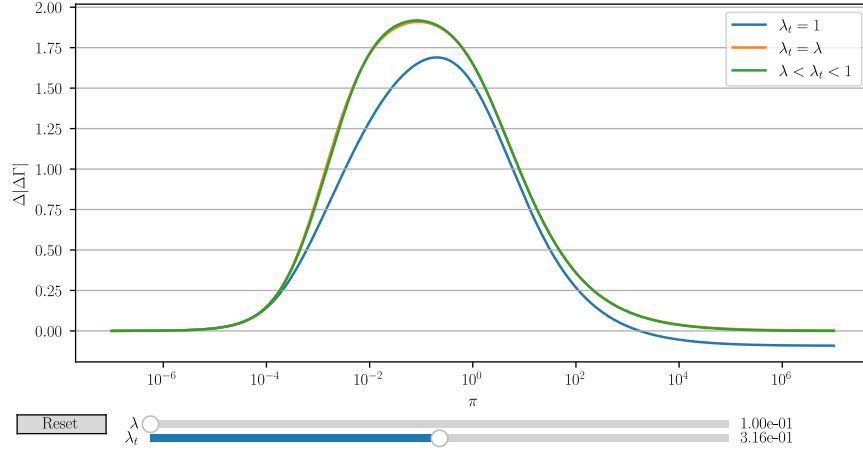
22

Figure 9: Improvement with respect to the non-kinetic case. The script generating these images can be found in the companion Github repository with the name `ImprovementsOfRp.py`

This behavior boils down to 3 quirks that appear on the plots, one for each, at high enough values of π. These oddities are, from left to right

- A local minimum appears in the left plot on all lines as early as $\pi = 3.09$ near $\lambda = 1$

- At $\pi \approx 1526$, the central plot with $\lambda_t = \lambda$ gets a sudden but small jump, caused by the next point in the list

- A second local maximum appears in the right plot with $\lambda_t = \lambda$, and at $\pi \approx 1526$ it surpasses the previous global maximum

We can easily find an explanation by looking at $\Delta\Gamma$ instead of $|\Delta\Gamma|$. When increasing π, the origin of the lines in the left plot of figure 8 shifts to the left, while the ends stay relatively similar, making the path curve to the center of the complex plane. Similarly, the closed path with $\lambda_t = \lambda$ in the right plot crosser over itself at $\pi \approx 66$, causing the second maximum to appear and at $\pi \approx 1526$, it surpasses the previous and causes the sudden rise in $|\Delta\Gamma(\pi)|$.

Finally, we can also see in figure 9 the improvement in each case, with the most being generally in between $\pi = 0.01$ and $\pi = 1$ and nearing a value of 2.

You can find all the scripts used for these simulations and the ones from section 4.1 in the Github repository for this project: JoseluMontoya/TFM.

5   Conclusions

We have been able to optimize the matching network attached to an SET. It turns out that for an optimum measurement, we need to tune the network for the geometric mean of the two resistances of the SET. These finding could prove extremely useful since, to my knowledge, analytical expressions for the optimum contrast and for the parameters that enabled that contrast were not derived up until now.

In addition to this, we showed that the use of a kinetic inductor improves greatly the quality of measurements, with the only recommendations for the implementation being:

- The larger the variation in inductance, the better

- The best tuning to use will depend on your restrictions: L_{On} tuning will be best if you need the lowest possible frequency, and you have some losses. If your concern is that you need a greater value of C_c, the middle tuning is perfect because, even though it uses a higher frequency than the L_{On} tuning, it needs the greatest C_c and the performance is better than the non-kinetic case for all values of π. Finally, if you want the best of the best (mostly when the losses practically non-existent, and you need a sliver of improvement), and you can afford a higher frequency and a small C_c, L_{Off} tuning is the best.

Due to the biggest improvements being around $\pi = 1$, I believe that the value of these finding lies in that the improvements of a kinetic inductance allow for bigger losses, and limit the circuit design a lot less.

6   Next steps and closing remarks

Some obvious next steps would be the experimental measurement of the optimum parameters we found and of the effect of the kinetic inductance.

Another good direction would be to try and obtain analytical expressions for the contrast with a kinetic inductance. This would allow us to gain a deeper knowledge, in the same vein as the optimization of the non-kinetic circuit.

Finally, an interesting idea to explore and formalize (credit to my supervisor for it, Fernando Gonzalez Zalba) is to design the kinetic inductance in such a way that, for the On state, the super conductance would brake, turning the inductor into a resistance (ideally high enough to not create a short circuit). Modifying the script used to generate figure 7 to plot this case, all tunings converge to the L_{Off}, but with an optimum C_c arbitrarily large for all cases. This case needs to be studied with more care and more formally, since it appears to be the definitive solution.

To end this thesis, I would like to thank my supervisor Fernando Gonzalez Zalba for all the guidance and help he gave me, and to my family and significant other for all the love and support.

References

[1] Guido Burkard, Thaddeus D. Ladd, John M. Nichol, Andrew Pan, and Jason R. Petta. Semiconductor Spin Qubits. 95(2):025003.

[2] D. P. DiVincenzo, D. Bacon, J. Kempe, G. Burkard, and K. B. Whaley. Universal quantum computation with the exchange interaction. 408(6810):339–342.

[3] M. F. Gonzalez-Zalba, prefix=de useprefix=true family=Franceschi, given=S., E. Charbon, T. Meunier, M. Vinet, and A. S. Dzurak. Scaling silicon-based quantum computing using CMOS technology. 4(12):872–884.

[4] George W. Hanson. *Fundamentals of Nanoelectronics.* Pearson/Prentice Hall.

[5] David J. Ibberson. Dispersive readout of industrially-fabricated silicon quantum dots.

[6] Jeremy Levy. Universal Quantum Computation with Spin- 1 / 2 Pairs and Heisenberg Exchange. 89(14):147902.

[7] Daniel Loss and David P. DiVincenzo. Quantum computation with quantum dots. 57(1):120–126.

[8] Yuli V. Nazarov and Yaroslav M. Blanter. *Quantum Transport: Introduction to Nanoscience.* Cambridge University Press.

[9] Florian Vigneau, Federico Fedele, Anasua Chatterjee, David Reilly, Ferdinand Kuemmeth, Fernando Gonzalez-Zalba, Edward Laird, and Natalia Ares. Probing quantum devices with radio-frequency reflectometry. 10(2):021305.

[10] Songyuan Zhao. Physics of Superconducting Travelling-Wave Parametric Amplifiers.